Hindawi
Geofluids
Volume 2021, Article ID 5549168, 9 pages
https://doi.org/10.1155/2021/5549168

Research Article

Numerical Simulation of Gas Ventilation Mode in Highway Gas Tunnel

Jihua Zhang[1], **Yun Dong**[1], **Yadong Chen**[1], **Huasheng Sun**[1], **Jingke Wu**[1], **Weili Liu**[2], **Jiarui Chen**[1] and **Shiqiang Pan**[3]

[1]*Faculty of Architecture and Civil Engineering, Huaiyin Institute of Technology, Huai'an, Jiangsu 223001, China*
[2]*School of Life Science and Food Technology, Huaiyin Institute of Technology, Huai'an, Jiangsu 223001, China*
[3]*Hunan Communications Research Institute Co., Ltd., Changsha, Hunan 410015, China*

Correspondence should be addressed to Jihua Zhang; zhangjh84@hyit.edu.cn

Received 8 January 2021; Revised 2 February 2021; Accepted 8 February 2021; Published 17 February 2021

Academic Editor: Yi Xue

When the mountain tunnel projects passing through the complex formation with coal, it happened along with disaster accidents such as gas outburst, gas combustion, and gas explosion. These disasters should seriously threaten the safety and life of the construction personnel and affect the normal operation of the tunnel construction. Ventilation is the most effective means to control gas, fire, dust, heat, and other disasters. To study the effects of different ventilation modes in highway gas tunnels, Fluent software was used to simulate forced ventilation, exhaust ventilation, and mixed ventilation in a high gas tunnel of a highway in Hunan. The distribution law of the airflow velocity and gas concentration of these three ventilation modes were obtained to determine the optimal ventilation system. It was shown that vortex zones of different ranges formed in the tunnel for all three ventilation modes, and the gas concentration was higher in the vortex zone than in other regions. Mixed ventilation of them is superior to the other two modes, showing the best ventilation effect with regard to airflow velocity and gas concentration.

1. Introduction

Currently, highway tunnel construction has expanded throughout China. Particularly with urban construction development, numerous traffic tunnels have arisen in the mountainous and hilly areas of China [1–3]. When these tunnel projects developing in depth, they often encounter the situation of crossing coal seam, which brings great security risks to tunnel construction. The tunnel is closed in the construction process, and the dust from driving and the blasting process and hazardous gases such as gas from the broken surrounding rock are likely to accumulate in the tunnel, which seriously threatens the safety of the workers [4–8]. Hence, adequate ventilation needs to be implemented in the tunnel [9–13] to dilute poisonous and hazardous gases in a timely manner and prevent the accumulation of explosive gases within the tunnel. Gas is a major risk source of tunnel construction safety. Because of the long ventilation distance and a large volume of gas emissions in a tunnel, ventilation via pipes is usually used to mitigate gas accumulation [14–17]. The study of the effects of different ventilation methods by pipes is critical for a reasonable selection of ventilation measures, improved ventilation efficiency, and a safe construction environment.

The tunnel studied here is in Jishou city, Hunan province, China. A coal seam was exposed during the excavation process, consisting of pork liver coal and asphaltic coal. These coals are tectonic coals, with high hardness and contain a large amount of gas with contents reaching 6.92 m^3/t. Furthermore, the methane concentration can reach 53.50% while the maximum absolute gas emission rate exceeds 75 m^3/min. After the exposure of the coal seam, the absolute gas emission rate exceeded 0.5 m^3/min for several consecutive days. According to "Technical Code for Railway Tunnel with Gas" and "Guidelines for Design of Highway Tunnel," together with the determination principle of the highest level in the tunnel gas work area, this tunnel was classified as a high gas tunnel. To guarantee the construction safety of this

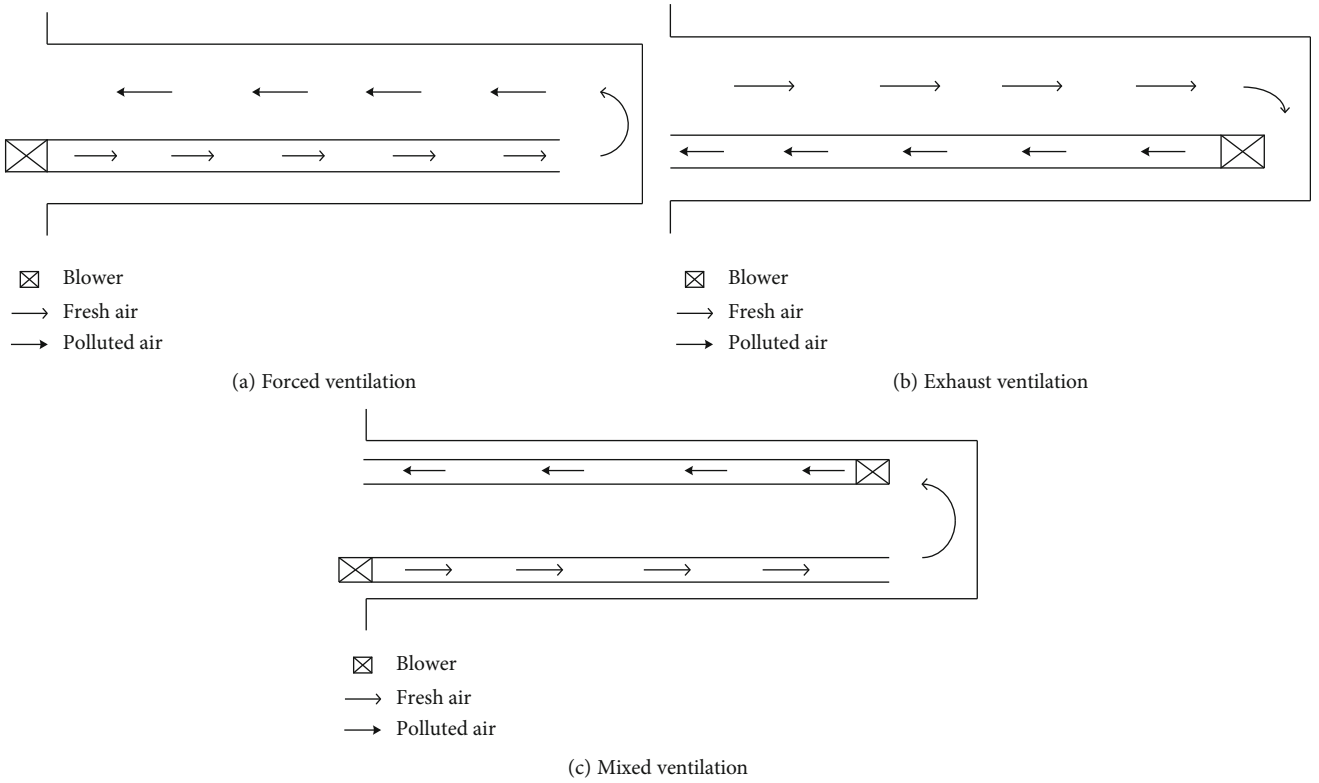

(a) Forced ventilation

(b) Exhaust ventilation

(c) Mixed ventilation

Figure 1: Schematic diagram of the ventilation model.

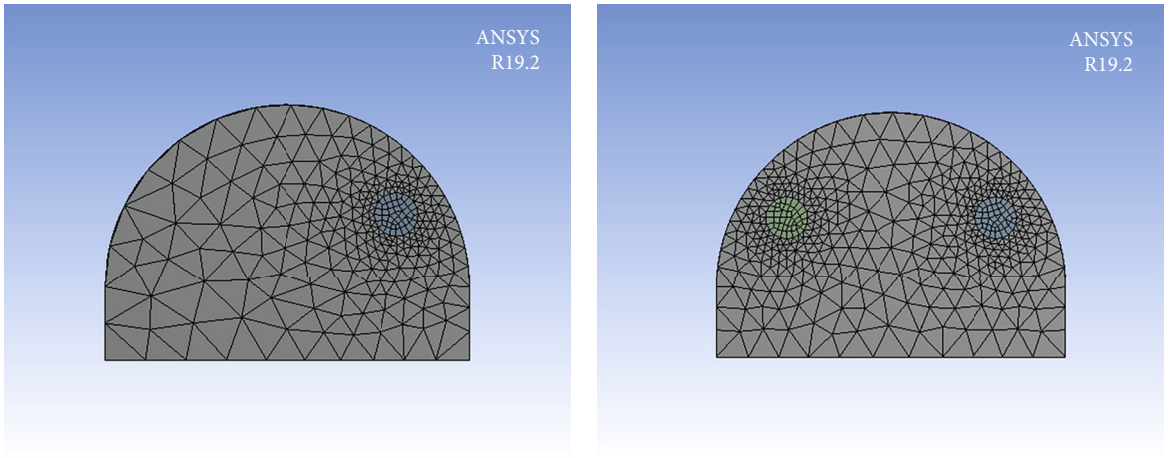

(a) Forced ventilation and exhaust ventilation

(b) Mixed ventilation

Figure 2: Schematic diagram of model meshing.

tunnel, effective measures of outburst prevention is necessary for penetration through the coal seam to suppress the gas concentration and gas pressure. This requires a scientific and rational configuration of the ventilation mode. Thus, in this paper, the hydrodynamics software Fluent was employed to simulate three different ventilation measures, forced ventilation, exhaust ventilation, and mixed ventilation, and the status of the transportation of fresh air and gas in different ventilation flow fields was obtained. Therefore, the efficiency of tunnel ventilation was able to be enhanced, and the safety of the workers was guaranteed using the results of this research.

2. Ventilation Modes of Air Pipe of Tunnel

In the driving construction of tunneling, ventilation by pipes can be divided into three types based upon the layout type of pipe and blower: forced ventilation, exhaust ventilation, and mixed ventilation [18–21]. When using forced ventilation, pipes deliver fresh air to the tunnel working face to suppress

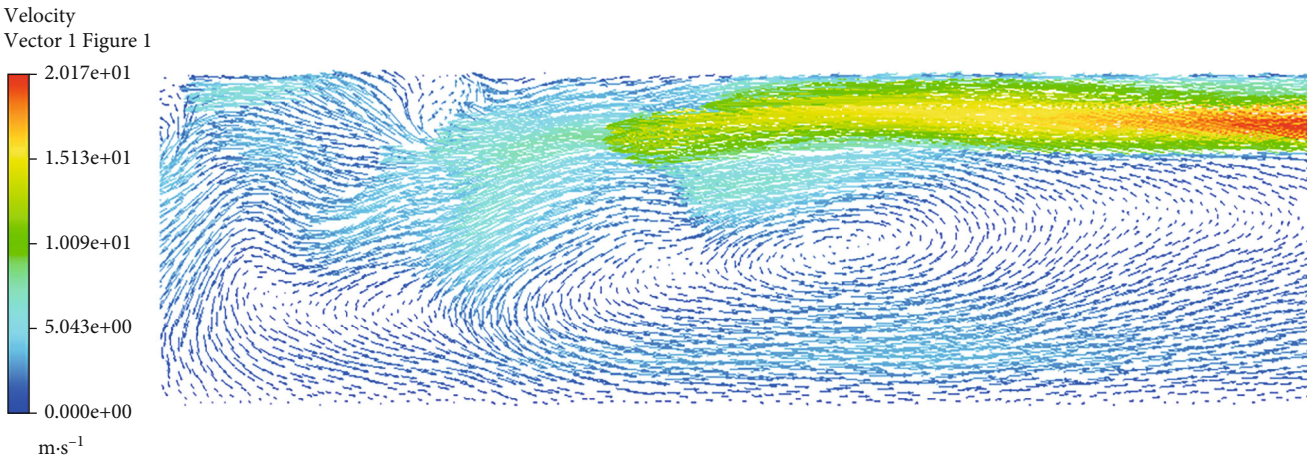

(a) Forced ventilation

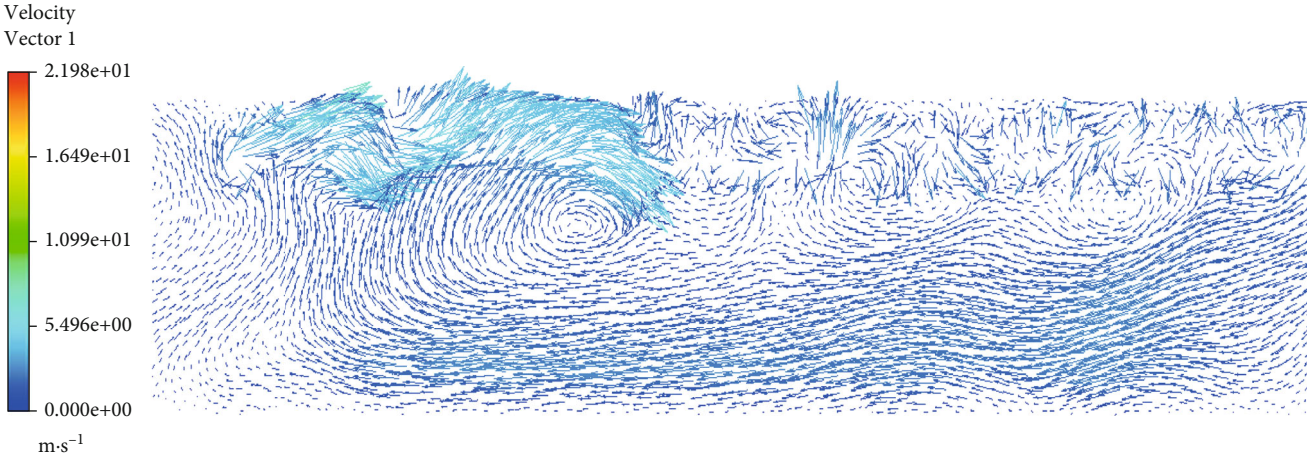

(b) Exhaust ventilation

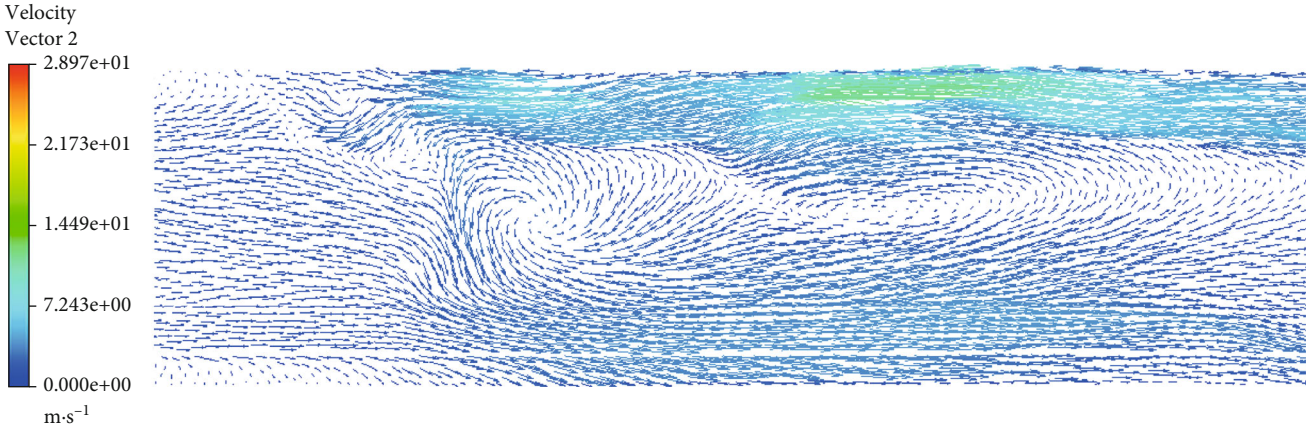

(c) Mixed ventilation

Figure 3: Wind flow velocity vector inside the tunnel.

the concentration of poisonous and hazardous gas in the air and discharge the polluted air through the tunnel portal. It has a short ventilation duration, an extensive effective range, and a favorable ventilation effect. Exhaust ventilation exhausts poisonous and hazardous gas at the tunnel's working face through negative-pressure pipes, provides fast ventilation, and is suitable for driving ventilation across a long tunnel. As a standard ventilation mode in tunnel construction, mixed ventilation uses a forced blower to dilute poisonous and hazardous gases at the working face and an exhaust blower to exhaust the polluted air through a ventilation pipe, which has the advantages of both the forced and exhaust ventilation modes so that the maximum ventilation efficiency can be

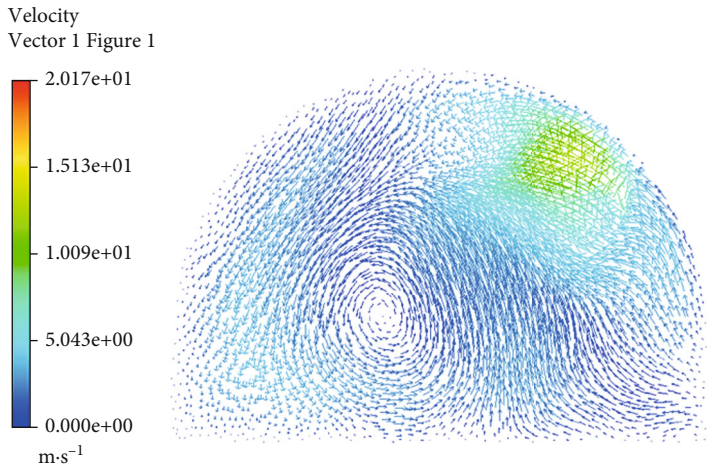

(a) Forced ventilation

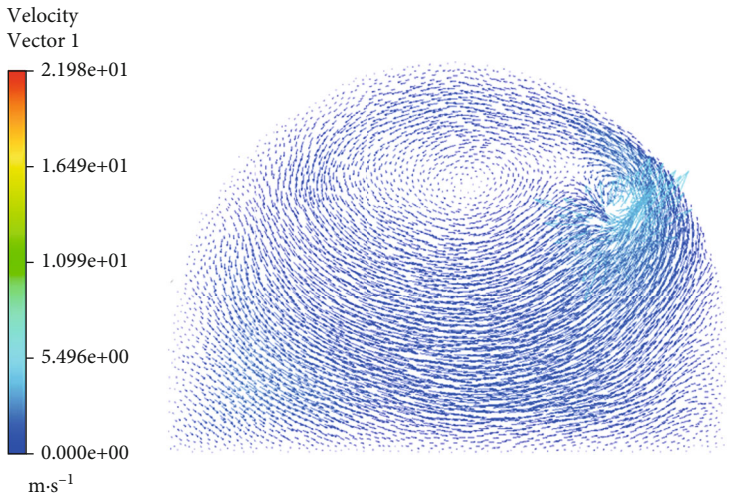

(b) Exhaust ventilation

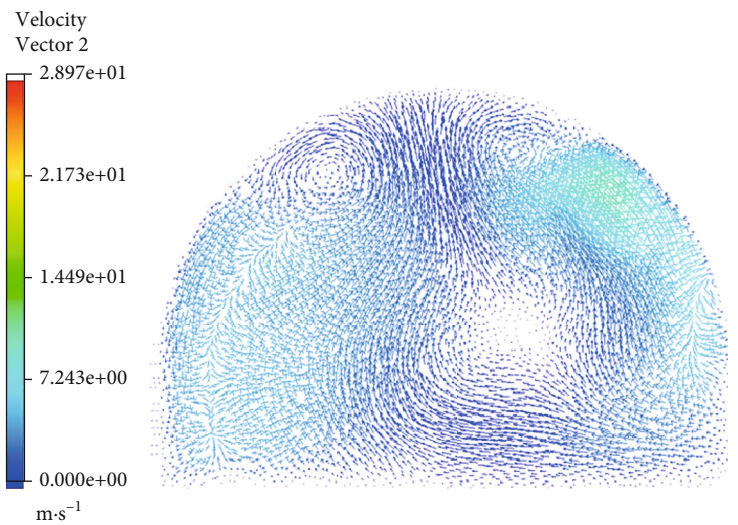

(c) Mixed ventilation

Figure 4: Tunnel section wind speed vector.

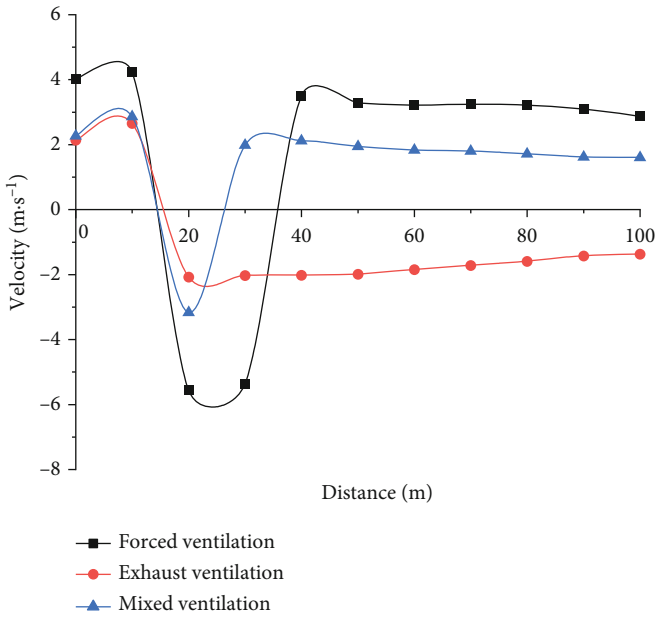

Figure 5: Curve of wind speed variation in the tunnel.

obtained, and it is especially suitable for ventilation of a long-distance tunnel.

3. Numerical Calculation Model

3.1. Calculation Model of Tunnel. The three-dimensional models of the three pipe ventilation modes of tunnel were established using Fluent software. The basic geometric dimensions of the tunnel were as follows: length was 100 m, cross-section was 10 m × 7 m straight wall circular arch (width × height), the diameter of the ventilation pipe was 1.2 m, and distance of pipe from the ground was 4 m. The tunnel ventilation model is simplified and shown in the schematic in Figure 1.

The mesh subdivision for the model was implemented by the preprocessor within Fluent software, and the generated mesh is shown in Figure 2.

3.2. Mathematical Model of Tunnel. When studying the airflow in the tunnel, the airflow was simplified as channel flow, and the airflow was modeled as nearly turbulent [22–26]. By referring to the tunnel ventilation condition, the $k-\varepsilon$ turbulence model was adopted in the calculation model [27–29], and thus, the $k-\varepsilon$ turbulence model was selected as the calculation model for gas diffusion [30–32]. The model solves the turbulent viscosity coefficient μ_i by establishing the equations of k and ε.

(1) Turbulent fluctuation kinetic energy equation (k equation)

$$\frac{\partial(\rho k v_i)}{\partial x_i} = \frac{\partial((\mu + (\mu_i/\sigma_k))(\partial k/\partial x_i))}{\partial x_i} + G_k - \rho\varepsilon, \quad (1)$$

where ρ is the fluid density, kg·m^{-3}; k is the turbulent kinetic energy, m^2·s^{-2}; v_i is the velocity component, m·s^{-1}; μ is the laminar viscosity coefficient, Pa·s; μ_i is the turbulent viscosity coefficient, Pa·s; σ_k is an empirical constant; G_k is the change rate of turbulent fluctuating kinetic energy caused by the change of average velocity gradient, which can be given by equation (2); ε is the turbulent kinetic energy dissipation rate, m^2·s^{-3}.

$$G_k = \mu_i \left(\frac{\partial v_i}{\partial x_j} + \frac{\partial v_j}{\partial x_i}\right) \frac{\partial v_i}{\partial x_j} \quad (i, j = 1, 2, 3) \quad (2)$$

(2) Turbulent fluctuation kinetic energy dissipation equation (ε equation)

$$\frac{\partial(\rho\varepsilon v_i)}{\partial x_i} = \frac{\partial((\mu + (\mu_i/\sigma_\varepsilon))(\partial\varepsilon/\partial x_i))}{\partial x_i} + C_1 \frac{\varepsilon}{k} G_k - C_2 \rho \frac{\varepsilon^2}{k}, \quad (3)$$

where σ_k, C_1, and C_2 are empirical constants

3.3. Calculation of Boundary Conditions. The boundary conditions were determined as follows:

(1) The ventilation pipe in the tunnel was set as the inlet boundary, which used the velocity-inlet with the ventilation velocity of 20 m/s

(2) The exhaust opening of the blower was set as the inlet boundary with the type of mass-flow inlet and $Q = 2.7$ m^3/s

(3) The walls of the tunnel and ventilation pipe were subject to a fixed wall boundary with nonslip conditions

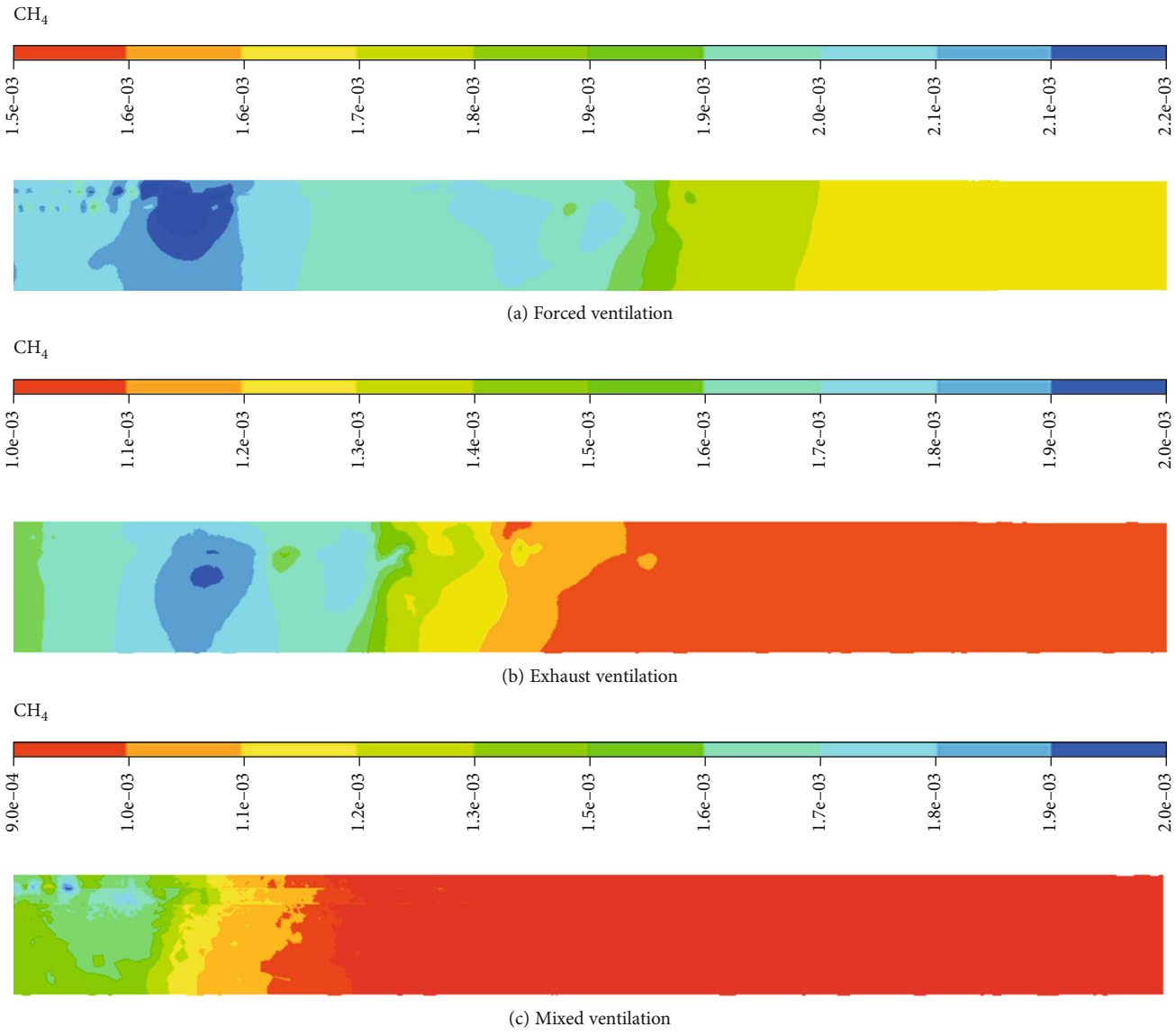

(a) Forced ventilation

(b) Exhaust ventilation

(c) Mixed ventilation

Figure 6: Distribution of gas concentration in the tunnel.

(4) Gas was emitted from the tunnel face with an emission rate of 0.5 m^3/min

4. Calculation Results and Analysis

4.1. Distribution of Airflow Velocity Field in the Tunnel. The tunnel face is the most likely location where gas is emitted and accumulated, and the ventilation effect of this location directly affects the ventilation status of the entire tunnel. Therefore, the local airflow field of the tunnel face is the focus of this numerical simulation study. To visually observe the distribution of the local airflow field in the tunnel, for the three ventilation modes, the velocity contours on the plane of the ventilation pipe center (plane $y = 4$ m) and the cross-section of the tunnel which was 5 m away from the tunnel face (plane $z = 5$ m) is analyzed as in Figures 3 and 4.

It can be observed in Figure 3 that in the forced ventilation, fresh air is delivered by the blower and the ventilation pipe to the tunnel face and lashes against the tunnel face; after mixing with the gas emitted through the tunnel face, the flow direction is altered due to rebounding on wall and backflow occurs towards the direction of the tunnel opening; a part of the airflow changes its direction under the effect of ventilation pipe opening jet flow and forms a vortex, and polluted air quickly accumulates in the vortex zone, which is the main factor influencing the exhaust of the polluted air. In exhaust ventilation, a suction region is formed around the blower, which sucks the gas emitted through the tunnel face and the air in the tunnel into the ventilation pipe for exhaustion from the tunnel. In the mixed ventilation mode, the airflow is delivered from the forced air pipe and mixed with gas, and then, the rotation of velocity occurs on the tunnel face so that most of the mixed gas is sucked into the ventilation pipe by the suction region formed by the blower before finally being exhausted out of the tunnel. It can be seen from the airflow velocity vectors on the tunnel cross-section

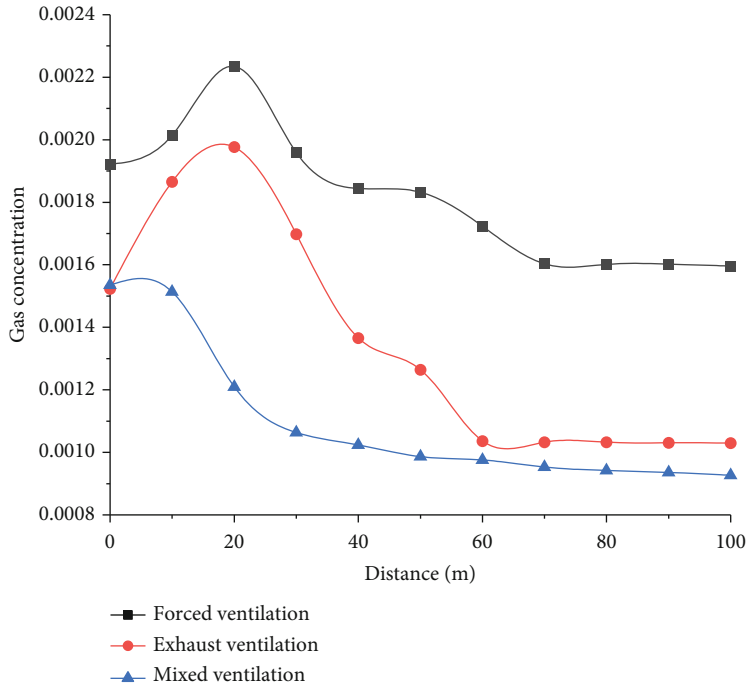

Figure 7: Variation curve of gas concentration in a tunnel under three ventilation modes.

in Figure 4 that for all three ventilation modes, the airflow velocity is always greater at the ventilation pipe and continuously dissipates out of the boundaries, and vortex zones of different sizes are produced for each three modes. Among them, the range of the vortex zone produced by mixed ventilation is relatively small. Overall, comparing the three ventilation modes: forced ventilation creates the most significant airflow velocity at the tunnel face. However, it is very likely to cause an extensive range of vortex zones in the ventilation pipe zone, resulting in gas accumulation; the airflow velocity of the exhaust ventilation is relatively small, which is against the gas exhaust and the inflow of fresh air; the airflow velocity is relatively large while the exhaust pipe exists in mixed ventilation, which enables the vectored flow of polluted air to the exhaust pipe, reducing the range of vortex zone and enhancing the ventilation efficiency.

To better understand the variation law of airflow velocity in a tunnel under the three ventilation modes, monitoring points for analyzing the airflow velocity variations were configured every 10 m along the tunnel centerline. The obtained airflow velocity variation curves are shown in Figure 5.

It can be observed in Figure 5 that for forced ventilation, the axial velocity of airflow 0~10 m from the tunnel face was around 4.1 m/s. The direction of the axial velocity of the airflow was altered at 15~35 m, resulting in airflow of -5.4 m/s. This indicates that a vortex zone formed in this region, in which airflow was subjected to rotational motion. Subsequently, the velocity direction was altered again, and finally, the polluted air was exhausted out of the tunnel at a constant velocity of 3.2 m/s. For exhaust ventilation, the axial velocity was 2.3 m/s in front of the tunnel face. The velocity decreased to -1.7 m/s at 15~30 m, and fresh air finally flowed into the tunnel at a velocity of -2.8 m/s. For mixed ventilation, the variation law of airflow velocity in the tunnel was similar to forced ventilation. From 0~10 m, the velocity was constant at 2.5 m/s and changed to -2.9 m/s at 15~25 m. The direction was then altered again. Finally, the air was exhausted out of the tunnel at a velocity of 1.8 m/s. It can be found by the velocity variations of the three ventilation modes that in the range of 15~30 m in front of the tunnel face, the airflow was inclined to form a vortex zone, which was likely to cause gas accumulation in the ventilation process. The range of the vortex zone can be derived by the range of the airflow velocity direction variation. Therefore, the range of the vortex zone was the largest in forced ventilation, followed by that in exhaust ventilation, and that in mixed ventilation was the smallest. This indicates that mixed ventilation showed the best ventilation efficiency.

4.2. Distribution Law of Gas Concentration in Tunnel. The study of the gas distribution law on the tunnel face is critical for the safe construction of a tunnel. Hence, the tunnel ($y = 0$ cross-section) center plane was selected to study the gas concentration distribution in a tunnel for the three ventilation modes. The obtained gas concentration distributions are shown in Figure 6.

Gas concentration monitoring points were located every 10 m along the tunnel's centerline, and the variation curves of gas concentration in the tunnel with distance were obtained for the three ventilation modes, as presented in Figure 7.

As shown in Figure 6, the gas concentration distributions tended to gradually decline along the direction from the opening of the ventilation pipe to the tunnel opening for all three ventilation modes. In the region where the ventilation pipe is located, a vortex formed due to the jet flow of the

ventilation pipe acting on the recirculated flow further caused an increase in local gas concentration. The gas concentration was distinctly higher in the vortex zone than in other regions. High gas concentration areas were concentrated in the vortex zone and the region of the ventilation pipe. It can be seen in Figure 7 that for both the forced ventilation and exhaust ventilation, the gas concentration values in the tunnel first increased, then decreased, and finally stabilized. The gas concentration maximums were mainly identified in the vortex zones 15~20 m in front of the tunnel face, which were 0.22% and 0.18%, respectively. In the range of 20~60 m from the working face, the gas concentration value fell to 0.16% and 0.11% and finally stabilized. However, for mixed ventilation, the gas concentration was high next to the tunnel face, and with an increase in distance, it gradually declined until it stabilized. At the region 0~5 m in front of the tunnel face, the gas concentration reached its maximum at 0.15%. In the range of 5~30 m, the concentration sharply dropped to 0.11% and then tended to stabilize. Among the three ventilation modes, mixed ventilation resulted in the lowest values for both the concentration of gas accumulation in the tunnel and the mean concentration of gas. Therefore, the ventilation efficiency of mixed ventilation was greater than that of the other two.

5. Conclusions

In this paper, the ventilation processes of three ventilation modes in a gas tunnel were simulated by Fluent software. Through the simulation, the three ventilation modes were studied in terms of the airflow's transportation law inside the tunnel, the distribution law of airflow velocity, and the distribution law of gas concentration in the tunnel. The following conclusions were addressed.

Vortex zones of different ranges were formed in the ventilation pipe region in the tunnel for all three ventilation modes. The existence of a vortex zone caused an accumulation of gas and affected the efficiency of ventilation. Thereinto, forced ventilation showed the most significant airflow velocity. However, the range of the vortex zone was also the greatest. The airflow velocity caused by the mixed ventilation mode was relatively great without any large-range vortex zones forming, which is beneficial for improving tunnel ventilation efficiency.

Between the recirculation zone and the vortex zone, the gas concentration distributions in the tunnel were obviously different between the three ventilation methods. The gas concentration was clearly higher in the vortex zone than in other areas. In terms of the concentration of gas accumulation region in the tunnel and the mean concentration of gas, mixed ventilation resulted in lower values than the other two and showed the greatest efficiency of ventilation.

Data Availability

The data used to support the findings of this study are available from the corresponding author upon request.

Conflicts of Interest

The authors declare that there are no conflicts of interest regarding the publication of this paper.

Acknowledgments

This work was supported by the National Natural Science Foundation of China (Nos. 51904112, 51904113, 51804129, 51808246, and 51708245), the Scientific and Technological Guidance Project of Jiangsu Construction System (Nos. 2018ZD268 and 2017ZD246), the Natural Science Foundation for Colleges and Universities in Jiangsu Province (No. 17KJB620002), and the Natural Science Foundation of Jiangsu Province (No. BK20170457), 2019 Huaishang Talent Plan Program (Project Principals Jiarui Chen).

References

[1] Y. Zhao and P. F. Li, "A statistical analysis of China's traffic tunnel development data," *Engineering*, vol. 4, no. 1, pp. 3–5, 2018.

[2] K. R. Hong and H. H. Feng, "Development trends and views of highway tunnels in China over the past decade," *China Journal of Highway and Transport*, vol. 33, no. 12, pp. 62–76, 2020.

[3] K. R. Hong, "Development and thinking of tunnels and underground engineering in China in recent 2 years (from 2017 to 2018)," *Tunnel Construction*, vol. 39, no. 5, pp. 710–723, 2019.

[4] Q. Z. Sun and B. J. Fan, "Stress analysis and movement study on construction tunnel dust," *Coal Technology*, vol. 35, no. 5, pp. 176–178, 2016.

[5] K. Wang and F. Du, "Coal-gas compound dynamic disasters in China: a review," *Process Safety and Environmental Protection*, vol. 133, pp. 1–17, 2020.

[6] P. Peng, Y. Fang, Y. C. Zhou, and X. G. Chen, "Effect analysis and parameter optimization of forced ventilation during tunneling," *Railway Standard Design*, vol. 58, no. 7, pp. 102–106, 2014.

[7] Y. Xue, P. G. Ranjith, F. Dang et al., "Analysis of deformation, permeability and energy evolution characteristics of coal mass around borehole after excavation," *Natural Resources Research*, vol. 29, no. 5, pp. 3159–3177, 2020.

[8] R. H. Lin, G. Q. Li, N. L. Hu, J. Gong, and H. Yang, "Parameters optimization of combined ventilation in an excavation roadway of high-altitude mine," *China Mining Magazine*, vol. 26, no. 4, pp. 121–125, 2017.

[9] P. Wu, Z. B. Feng, S. J. Hu, and J. Cao, "Fast and accurate prediction of airflow and drag force for duct ventilation using wall-modeled large-eddy simulation," *Building and Environment*, vol. 141, no. 8, pp. 226–235, 2018.

[10] W. B. Ye, "Design method and modeling verification for the uniform air flow distribution in the duct ventilation," *Applied Thermal Engineering*, vol. 110, pp. 573–583, 2017.

[11] Y. D. Huang, X. L. Gong, Y. J. Peng, and C. N. Kim, "Effects of the solid curtains on natural ventilation performance in a subway tunnel," *Tunnelling and Underground Space Technology*, vol. 38, no. 9, pp. 526–533, 2013.

[12] E. Mostafa, I. B. Lee, S. H. Song et al., "Computational fluid dynamics simulation of air temperature distribution inside broiler building fitted with duct ventilation system," *Biosystems Engineering*, vol. 112, no. 4, pp. 293–303, 2012.

[13] Y. D. Huang, W. Gao, and C. N. Kim, "A numerical study of the train-induced unsteady airflow in a subway tunnel with natural ventilation ducts using the dynamic layering method," *Biosystems Engineering*, vol. 22, no. 2, pp. 164–172, 2010.

[14] G. M. Xie, "Research on ventilation technology of high gas tunnel," *Highway Engineering*, vol. 43, no. 3, pp. 263–267, 2018.

[15] X. Zhao, S. Q. Li, and F. Huang, "Advanced detection of coal seam and methane detection in highway gas tunnel," *Highway Engineering*, vol. 44, no. 4, pp. 163–168,173, 2019.

[16] R. X. Li, H. W. Chen, S. Y. Zhou, and X. P. Liu, "Analysis on the genesis of gas in the tunnel with oil and gas and its safety management," *Modern Tunnelling Technology*, vol. 56, no. 6, pp. 36–40,46, 2019.

[17] Z. Y. Zhou, P. Hu, Z. C. Han, and J. H. Chen, "Effect of heading face ventilation arrangement on regulation of dust distribution," *Journal of Central South University(Science and Technology)*, vol. 49, no. 9, pp. 2264–2271, 2018.

[18] P. P. Cheng, H. N. Wang, L. Mi, Q. C. Liang, and J. Gao, "3D simulation on transporting of particle dust in horizontal duct," *Chinese Journal of Environmental Engineering*, vol. 11, no. 10, pp. 5457–5464, 2017.

[19] P. Ntzeremes and K. Kirytopoulos, "Evaluating the role of risk assessment for road tunnel fire safety: a comparative review within the EU," *Journal of Traffic and Transportation Engineering(English Edition)*, vol. 6, no. 3, pp. 282–296, 2019.

[20] R. Hansen, "Fire behaviour of multiple fires in a mine drift with longitudinal ventilation," *International Journal of Mining Science and Technology*, vol. 29, no. 2, pp. 245–254, 2019.

[21] A. T. Zhou, K. Wang, L. G. Wu, and Y. W. Xiao, "Influence of gas ventilation pressure on the stability of airways airflow," *International Journal of Mining Science and Technology*, vol. 28, no. 2, pp. 297–301, 2018.

[22] X. B. Kang, S. Luo, Q. S. Li, M. Xu, and Q. Li, "Developing a risk assessment system for gas tunnel disasters in China," *Journal of Mountain Science*, vol. 14, no. 9, pp. 1751–1762, 2017.

[23] H. Rickard, "Fire behavior of mining vehicles in underground hard rock mines," *International Journal of Mining Science and Technology*, vol. 27, no. 4, pp. 627–634, 2017.

[24] J. Li, T. Yu, X. Liang, P. Zhang, C. Chen, and J. Zhang, "Insights on the gas permeability change in porous shale," *Advances in Geo-energy Research*, vol. 1, no. 2, pp. 69–73, 2017.

[25] Y. Zhao, S. Chen, X. Tan, and M. Hui, "New technologies for high-risk tunnel construction in Guiyang-Guangzhou high-speed railway," *Journal of Modern Transportation*, vol. 21, no. 4, pp. 258–265, 2013.

[26] A. Bond, S. Benbow, J. Wilson et al., "Reactive and non-reactive transport modelling in partially water saturated argillaceous porous media around the ventilation experiment, Mont Terri," *Journal of Rock Mechanics and Geotechnical Engineering*, vol. 5, no. 1, pp. 44–57, 2013.

[27] J. C. Fang, C. D. Zhang, Z. Z. Gou, and B. He, "Analysis of three dimensional dynamic numerical simulation of the construction ventilation of long tunnel," *Highway Engineering*, vol. 42, no. 1, pp. 139–142,155, 2017.

[28] Y. Xue, F. Gao, Y. Gao, X. Liang, Z. Zhang, and Y. Xing, "Thermo-hydro-mechanical coupled mathematical model for controlling the pre- mining coal seam gas extraction with slotted boreholes," *International Journal of Mining Science and Technology*, vol. 27, no. 3, pp. 473–479, 2017.

[29] C. P. Xin, F. Du, K. Wang, C. Xu, S. G. Huang, and J. T. Shen, "Damage evolution analysis and gas–solid coupling model for coal containing gas," *Geomechanics and Geophysics for Geo-energy and Geo-resources*, vol. 7, no. 7, pp. 1–15, 2021.

[30] C. F. Wu, B. Jin, Z. Y. Chen, and Y. Liu, "Numerical simulation on combined ventilation in excavation roadway," *Nonferrous Metals(Mine Section)*, vol. 67, no. 1, pp. 69–73,82, 2015.

[31] W. Shen, X. Li, A. Cihan, X. Lu, and X. Liu, "Experimental and numerical simulation of water adsorption and diffusion in shale gas reservoir rocks," *Advances in Geo-energy Research*, vol. 3, no. 2, pp. 165–174, 2019.

[32] T. T. Long, K. P. Zhou, Q. F. Chen, and J. L. Li, "A simulated study on the ventilation effect of the heading face based on PMV index," *Journal of Safety and Environment*, vol. 8, no. 3, pp. 122–125, 2008.